2011-09

Polyfluorene based blends for white light emission

Organic Electronics, Amsterdam : Elsevier BV, v. 12, n. 9, p. 1493-1504, Sept. 2011
http://www.producao.usp.br/handle/BDPI/50046

Organic Electronics 12 (2011) 1493–1504

Contents lists available at ScienceDirect

Organic Electronics

journal homepage: www.elsevier.com/locate/orgel

Polyfluorene based blends for white light emission

Jeferson Ferreira de Deus [a,b], Gregório C. Faria [c], Eduardo T. Iamazaki [d], Roberto M. Faria [c], Teresa D.Z. Atvars [d], Leni Akcelrud [e,*]

[a] Programa de Pós-graduação em Engenharia de Materiais e Processos – PIPE, Universidade Federal do Paraná, Curitiba, PR, Brazil
[b] Universidade Tecnológica Federal do Paraná, Curitiba, PR, Brazil
[c] Instituto de Física de São Carlos, São Carlos, SP, Brazil
[d] Instituto de Química, Universidade Estadual de Campinas, Campinas, SP, CEP 13084-971, Brazil
[e] Laboratório de Polímeros Paulo Scarpa – LaPPS, Departamento de Química, Universidade Federal do Paraná, Caixa Postal 19081-990, CEP 81531-990, Curitiba, PR, Brazil

ARTICLE INFO

Article history:
Received 18 January 2011
Received in revised form 3 April 2011
Accepted 10 April 2011
Available online 25 June 2011

Keywords:
Photoluminescence
Electroluminescence
Polymer blends
White device emission

ABSTRACT

Single layer white light emitting diodes were constructed with blends containing as blue emitter and matrix host poly(9,9-dihexyl-2,7-fluorene) (LaPPS10), and the green and red emitters poly[(9,9-dihexyl-9H-fluorene-2,7-diyl)-1,2-ethenediyl-1,4-phenylene-1,2-ethenediyl] (LaPPS16) and poly[2-methoxy-5-(2-ethylhexoxy)-1,4-phenylene vinylene] (MEH-PPV), respectively, as guests components. Two blends were studied: LaPPS10:LaPPS16:MEH-PPV = 100:0.01:0.20 (w/w) (JF14) and another with the same components and a second blue emitter: a copolymer of poly(methyl methacrylate-*co*-methyl antracenyl methacrylate), P(MMA-*co*-MMAnt), with the composition LaPPS10:P(MMA-*co*-MMAnt):LaPPS16:MEH-PPV = 100:40:0.01:0.20 (w/w) (JF17). The PL spectra of JF14 and JF17 in the higher energy edge are characteristic of the matrix (LaPPS 10). The morphological characterization showed the formation of a biphasic structure with a matrix of LaPPS10 and segregated domains of MEH-PPV in the case of JF14 and of P(MMA-*co*-MMAnt) in the case of JF17. Significant differences between EL and PL spectra were observed for the blends indicating that the mechanism for the excited states or quenching processes are very different in both cases. In addition, the EL emissions suggested that the cascade mechanism for the charge migration or charge recombination or energy transfer processes are also incomplete allowing more than one type of emission. EL spectra were red-shifted in relation to PL, which was partly attributed to the trapping of energy carriers that may occur in EL, apart from energy transfer. The CIE coordinates for EL emission of JF14 blend the coordinates are (0.30, 0.32) and for JF17 blend are (0.29, 0.38) corresponding to white light emission. Spectroscopic data brought evidence of the formation of the β phase in the polyfluorene matrix, and due to differences in band gap, it was concluded that hole carriers tend to be injected into that phase rather than into the disordered one, leading to the proposal that EL emission was predominantly originated from the β phase.

1. Introduction

White organic light emitting diodes (WOLEDs) are one of the most important developments in the field of polymer emitting devices, mainly due to their applications in solid-state lighting and flat-panel displays [1,2]. To achieve white light emission two complementary colors (blue and orange) or the three primary colors have to be produced simultaneously [3]. In general, organic molecules show broad emission spectra and the combination of not exactly complementary colors can present a white light output [4]. In this line of pursuit, several approaches have

* Corresponding author.
E-mail address: leni@ufpr.br (L. Akcelrud).

1566-1199/$ - see front matter © 2011 Elsevier B.V. All rights reserved.
doi:10.1016/j.orgel.2011.04.022

been reported, including the mixing of polymers with different emission colors in single or multilayer devices, or the blending of small molecules in a appropriate ratio of red, green and blue (RGB), host–guest systems, in single or multiple layers [3,5–10]. The doping with phosphorescent complexes or fluorescent dyes in a polymer matrix or small molecule host exciplexes in bilayer devices or still a single polymer with different chromophores have also been reported [5,11–13].

The main issue for achieving white light through the blending of two or more chromophoric materials is the energy transfer among the various components. This energy transfer has to be incomplete, since all the colors should appear in the electroluminescence spectrum, requiring a judicious control in the concentration balance and miscibility of the mixture materials [14,15]. The basic operating mechanism involves the charge carriers injection, a partial energy transfer in order to avoid cascade non-radiative decays that will lead only to the lower-laying emission from the excited state [16,17]. The selected color in the donor–acceptor system is obtained by setting the appropriate dopant concentration. The range of dopant variation is limited, usually less than 1% and 10% for fluorescent and phosphorescent materials, respectively [10]. The upper limit is dictated by aggregate formation; since higher amounts lead to non-radiative self-quenching or intermolecular energy transfer processes [3,17]. Electroluminescent polymer blends are systems containing at least one active material which generally presents a better performance as compared to the material itself [18]. This effect can be explained by the synergic contribution of several factors, including the de-aggregation of associated species in the active medium (as ground state dimmers or excimers), the presence of heterojunctions between polymeric phases, improvement of the interfacial adhesion and of the optical properties, etc. These factors contribute to higher efficient exciton formation, charge transport and charge recombination [18–21]. When two or more active materials are blended, color tunability can also be obtained [19,20].

In this work a single layer device was explored, in which the blue emitter [poly(9,9-dihexyl-2,7-fluorene)] (LaPPS10) is the matrix host, and the green and red emitters poly[(9,9-dihexyl-9H-fluorene-2,7-diyl)-1,2-ethenediyl-1,4-phenylene-1,2-ethenediyl] (LaPPS16) and poly [2-methoxy-5-(2-ethylhexoxy)-1,4-phenylene vinylene] (MEH-PPV), respectively, were the guest components. The performance of this blend was compared with another using a second blue component, a copolymer of poly (methyl methacrylate-*co*-methyl antracenyl methacrylate), P(MMA-*co*-MMAnt) that was responsible by the improvement of the optical quality of the material [22]. The chemical structures are depicted in Fig. 1.

The choice of a polyfluorene for the main component was based on the fact that this class of polymer has emerged as an important class of blue emitter, with intense photoluminescence, good charge transport and thermal stability properties [23–26]. The other components, all of them also electroluminescent in a different spectral range, were chosen as an attempt to achieve white light emission. White light electroluminescent devices with organic materials can be built in multi-layer configuration composed by several different materials where each layer emits in a different region of the visible spectrum, generating white light output [27]. Here, single-layer devices were built, using blends with emitting materials of different band gap energies, exploring partial energy transfer [28]. Single layer devices are more attractive due to its ease of fabrication, large scale production and cost effective features, and according to published data they are more stable than those built with emitters in separated layers [20,29–31]. Therefore, for a system where the emission of one material spectrally overlaps with the absorption of another, a separating material had to be incorporated into the blend so as to prevent complete energy transfer and to give white emission with a wide spectral range [32]. To achieve this goal, morphology control of the polymer film is a crucial step and plays a main role on the device performance.

2. Experimental

2.1. Materials

The light emitting polymers poly(9,9-dihexyl-2,7-fluorene) (LaPPS10) poly[(9,9-dihexyl-9H-fluorene-2,7-diyl)-1,2-ethenediyl-1,4-phenylene-1,2-ethenediyl] (LaPPS16), poly(methylmethacrylate-*co*-methyl-antracenyl methacrylate P(MMA-*co*-MMAnt) (molar composition of 35:1 of MMA:MMAnt) were synthesized in our laboratory (LaPPS) as described in previous papers [20,22,33]. MEH-PPV was used as purchased from Sigma–Aldrich. Structures are in Fig. 1. The solvent chloroform (Vetec) was used without further purification. The solutions were mixed in different ratios, according to the blend's composition desired. LaPPS10:LaPPS16:MEH-PPV = 100:0.01:0.20 (w/w) (JF14) and LaPPS10:P(MMA-*co*-MMAnt):LaPPS16:MEH-PPV = 100:40:0.01:0.20 (w/w) (JF17). Blends were formed by casting from chloroform solutions and dried at room temperature for several days.

2.2. Samples for photophysical measurements

LaPPS10, LaPPS16, P(MMA-*co*-MMAnt) and MEH-PPV were dissolved in chloroform separately, in 10^{-5} mol L^{-1} concentration. Films were obtained from the solutions filtered through 0.2 μm Millex-FGS Filters (Millipore Co.), deposited by casting on quartz plates and allowed to dry slowly in a controlled solvent ambient. The film's thickness was adjusted in order to assure optical behavior according to Beer's Law.

2.3. Device preparation

The EL device fabrication with the configuration ITO/PEDOT-PSS/emissive layer/Al followed the procedure: the substrates were cleaned with detergent, acetone and isopropyl alcohol and subsequently underwent a process of hydrophylization with plasma ozone. Next a layer of PEDOT-PSS (Bayer) was deposited by spin coating at a speed of 4000 rpm, resulting in a 60 nm thick layer. The

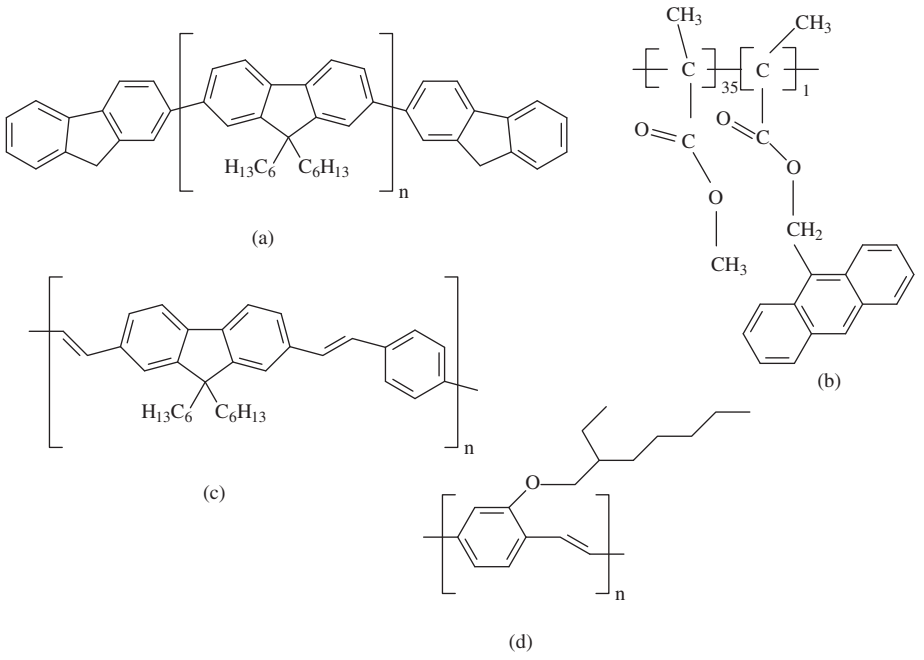

Fig. 1. Chemical structures of the emitting polymers: (a) LaPPS10 (blue), (b) P(MMA-*co*-MMAnt) (blue), (c) LaPPS16 (green) and (d) MEH-PPV (red). (For interpretation of the references to color in this figure legend, the reader is referred to the web version of this article.)

components of each material (polymer blend, JF14 and JF17) were dissolved in chloroform, with 25 mg/mL concentration. Films were obtained from the solutions filtered through 0.2 μm Millex-FGS Filters (Millipore Co.), deposited by spin coating using a rotation of 3000 rpm, forming films of 70 nm. The aluminum cathode was vacuum-deposited onto the blend layer under a pressure of about 10^{-6} mbar resulting in a layer 100 nm thick, completing the device preparation. The two devices are also named JF14 and JF17, according to their blends.

2.4. Optical analyses

UV–vis spectra were recorded on a Shimadzu model UV 2401 PC spectrophotometer, single beam, in the range of 250–750 nm. Steady-state emission spectra were acquired in a Shimadzu 5301 PC spectrofluorimeter, in the visible range of 390–780 nm. A 1.0 cm quartz square cuvette was used for solutions and a home-made optical support for film samples.

Fluorescence decays were recorded using time correlated single photon counting in an Edinburg Analytical Instruments FL 900 spectrofluorimeter using a pulsed hydrogen lamp, in a frequency rate of 40 kHz. Measurements were performed with wavelength excitation of λ_{exc} = 320 nm and the emission signals were collected in λ_{em} = 440 nm, respectively for solutions and for films. The sample cuvette was evacuated for 15 min and sealed under vacuum. The sample decay signal was deconvoluted from the lamp signal using the scattering from a Ludox® sample. The experimental curves were fitted using the software F900 provided by Edinburg. The analysis was performed by fitting the decays with multiple exponential functions using non-linear least-squares routines minimizing the χ^2. Good fits were obtained when χ^2 is close to 1.

$$I(t) = B_1 \exp\left(\frac{-t}{\tau_1}\right) + B_2 \exp\left(\frac{-t}{\tau_2}\right) + B_3 \exp\left(\frac{-t}{\tau_3}\right) + \ldots \quad (1)$$

τ_i is the fluorescence lifetime, B_i is the corresponding pre-exponential term and represents the contribution of each decay time to the total curve.

Epifluorescence optical images were recorded in a Leica DM IRB inverted microscope operating with a mercury lamp for UV–vis excitation in the transmission configuration. Pairs of optical filters for excitation and emission (dichroic mirrors) were selected in the range of λ_{exc} = 330–380 nm and λ_{em} > 440 nm, respectively. Photomicrographs were recorded using two microscope configurations: epifluorescence using UV-excitation and epifluorescence combined with lamp transmission to improve the image contrast. In this last configuration small bright domains could be visualized.

The CIE coordinates were calculated from data taken from the EL or PL emission, using the software CIE 31 xyz.xls.

2.5. Electroluminescence spectra, JxV and LxV measurements

The current–voltage measurements were performed using a 2400 Keithley Source. The EL spectra were acquired using a Labsphere Diode Array Spectrometer 2100 connected with Labsphere System Control 5500. The luminance–voltage was measured by 238 Keithley connected with a sensible photodiode. The samples were kept in a sealed Janis chamber with high vacuum.

3. Results and discussion

3.1. Photoluminescence properties

3.1.1. Solution properties

Fig. 2 presents the absorption and emission spectra of each polymer separately, recorded from the respective chloroform solutions (10^{-5} mol L^{-1}). Absorption of the P(MMA-*co*-MMAnt) is composed by a well defined vibronic structure in the range from 300 to 398 nm, characteristic of the anthracenyl moieties with the 0–0 band centered at $\lambda_{abs(0-0)}$ = 387.8 nm, and emission with the 0–0 band centered at $\lambda_{em(0-0)}$ = 393 nm [22,34,35]. Considering the 0–0 band for both absorption and emission, the Stokes shift is 341 cm^{-1}.

The LaPPS10 absorption band is broad and centered at $\lambda_{abs(0-0)}$ = 378.2 nm, strongly overlapped with that of P(MMA-*co*-MMAnt). Differently of the absorption, the LaPPS10 emission has a well resolved vibronic structure, with the 0–0 band at $\lambda_{em(0-0)}$ = 415.8 nm. The Stokes-shift taken as the difference between the absorption maximum and the 0–0 band of the emission is 2391 cm^{-1}. Absorption and emission spectra were not mirror images, indicating that the emission arises from a relaxed Franck–Condon state and are provided by energy transfer or by energy migration processes [37]. The LaPPS16 absorption band is also broader, two maxima were observed in the vibronic structure, at 430 nm and $\lambda_{abs(0-0)}$ = 454 nm. Its fluorescence emission has a partially resolved vibronic structure with the 0–0 band at $\lambda_{em(0-0)}$ = 472 nm. The Stokes-shift considering the 0–0 band in the absorption and emission spectra is 840 cm^{-1}. This smaller Stokes-shift suggests that Franck–Condon states with similar geometry are involved in the ground and electronic excited states due to the more rigid structure composed by a sequence of fluorene–vinylene alternated groups.

The MEH-PPV absorption band is also broader and centered at λ_{abs} = 491.5 nm. Emission is centered at $\lambda_{em(0-0)}$ = 554 nm, with a Stokes-shift of 2295 cm^{-1}. Therefore, taking this set of individual polymers, the absorption bands range from 325 to 550 nm, and the photoluminescence bands in solution that appears in the 400–600 nm range, cover almost the entire visible region.

3.1.2. Film properties

Fig. 3 presents the absorption and emission spectra of each component in the solid state. The P(MMA-*co*-MMAnt) absorption is composed by a well resolved vibronic

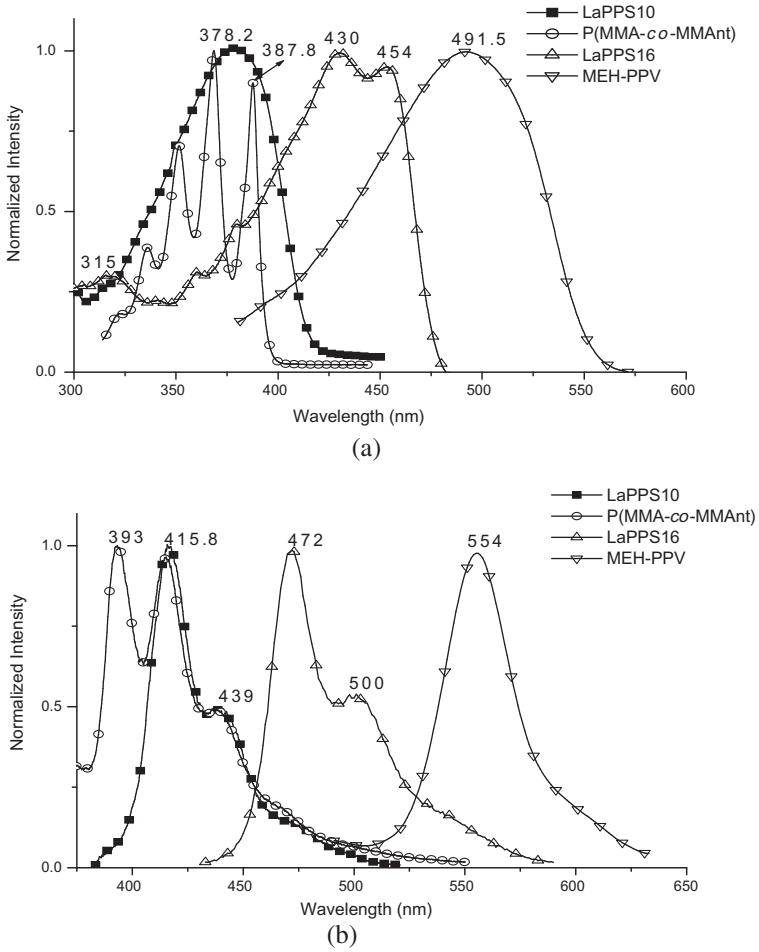

Fig. 2. Electronic absorption (a) and fluorescence (b) spectra of the polymers in 10^{-5} mol L^{-1} chloroform solutions. All samples were excited at λ_{exc} = 380 nm.

structure in the range of 300–420 nm, characteristic of the anthracenyl moieties, with the 0–0 band centered at $\lambda_{abs(0-0)}$ = 390.2 nm [22,34,35]. This spectrum is broader and red-shifted by 2.5 nm compared to the dilute solution. The lower energy peak at $\lambda_{abs(0-0)}$ = 410.4 nm can be attributed to ground state aggregates. Its emission is also broader with the 0–0 band centered at $\lambda_{em(0-0)}$ = 421.8 nm with a maximum located around 442.8 nm and

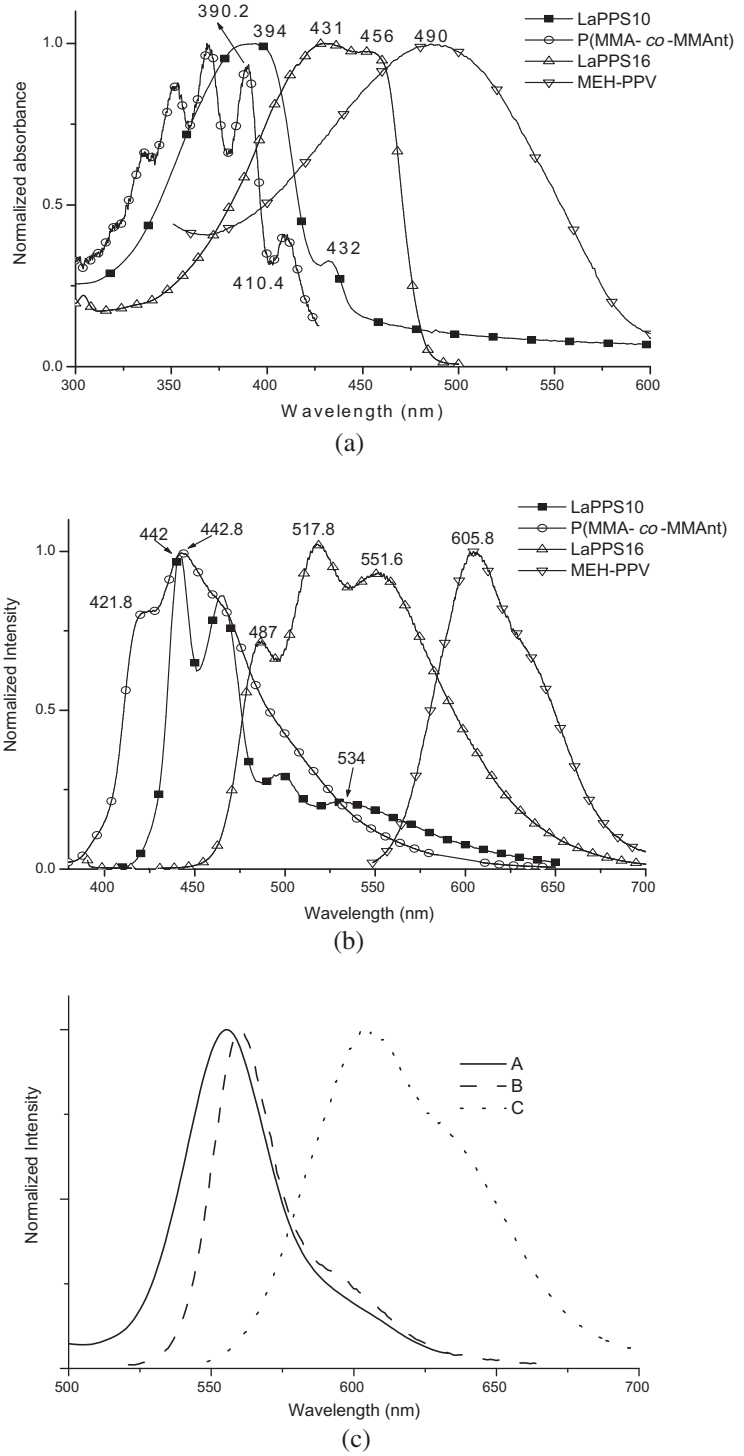

Fig. 3. Electronic absorption (a) and fluorescence (b) spectra of the polymers in film form. LaPPS10, LaPPS16 and P(MMA-*co*-MMAnt) were excited with λ_{exc} = 380 nm and MEH-PPV was excited with λ_{exc} = 490 nm. (c) Progresses red shift MEH-PPV emission with concentration, chloroform solutions (A) 10^{-7} mol L^{-1}, (B) 10^{-5} mol L^{-1} and (C) film.

with a Stokes-shift of 1920.0 cm^{-1}. The emission band has a red-edge tail, due to the presence of anthracenyl aggregates [22]. Generally, the presence of broad emission bands can be attributed to conformational disorders of the polymer chains where differences of microenvironment around every lumophore modifies their state densities [34]. Due to the large distance between two anthracenyl groups bonded to the main chain (35 MMA units) no excimer or aggregate emissions were observed in diluted solutions, and thus we ascribed the red-edge emission tail to aggregation of the lumophores in the solid state [34]. Emission of anthracenyl aggregates has been described and their formation requires very specific orientation of the polymer chains [37].

The LaPPS10 absorption band is broad and centered at λ_{abs} = 394 nm, red-shifted by 16 nm compared to the dilute solution. The presence of the low intensity band at λ_{abs} = 432 nm is a strong evidence that during the film formation some chains or chains segments are arranged in the β-conformation, a more planar orientation of the backbone [36,38–41]. The differences in the emission spectra of the blue emitter LaPPS10 in solution and in film form give further support for the presence of the β phase. The emission has a well resolved vibronic structure, with the 0–0 band at $\lambda_{em(0-0)}$ = 442 nm, with a Stokes-shift of 2756 cm^{-1}, red-shifted compared with the spectrum in solution by 27 nm. The emission in films of polyfluorenes in the 440 nm region has been assigned to the β-phase, and since its band gap is smaller than that of amorphous polymer, it may act as acceptors of resonance energy transfer [42]. That could be in part responsible for the absence of the higher energy bands seen in dilute conditions. The additional red-edge emission band at λ_{em} = 534 nm is characteristic of the LaPPS10 aggregates [41].

The LaPPS16 absorption band is also broader, with a poor resolved vibronic structure with two maxima at λ_{abs} = 431 nm and $\lambda_{abs(0-0)}$ = 456 nm. Its fluorescence emission is much broader than that in solution with the 0–0 band at $\lambda_{em(0-0)}$ = 487 nm, red-shifted by 15 nm compared to the dilute solution. In addition, two other strong bands at 517.8 and 551.6 nm are observed, possibly originated from aggregates [41]. Further, the LaPPS16 aggregate emission has a greater contribution to its total emission than that observed for LaPPS10.

The MEH-PPV absorption band is also broader compared to the solution and centered at $\lambda_{abs(0-0)}$ = 490 nm. Again, this spectral broadening can be ascribed to the inhomogeneous broadening in solid state produced by a larger distribution of states of individual chains in addition to the chain aggregation in more ordered regions. Its photoluminescence spectrum is not as broader as the absorption and centered at λ_{em} = 605.8 nm in the solid state, red-shifted by 52 nm compared to the solution spectra, with a larger Stokes-shift of 3985 cm^{-1}. Because of the relatively sharper and strongly red-shifted photoluminescence we suggest that its emission is occurring in more aggregated domains [43].

Putting all the individual absorption profiles together, we can see that they cover practically the entire visible spectral range (including part of the UV) whereas the photoluminescence ones also cover the entire visible spectrum, from the violet to the red (400–700 nm). Additionally, it can be seen from Fig. 3 that there is a strong overlap between the absorption from LaPPS16 and the photoluminescence from both LaPPS10 and P(MMA-*co*-MMAnt), as well as the absorption from MEH-PPV and the photoluminescence from LaPPS16. These spectral overlaps among the absorption and emission of the blend components play an important role on the photophysical properties of their polymer blends, since this is an important requirement for the resonant energy transfer process [44].

Fig. 4 shows the absorption and emission spectra of the blends: LaPPS10:LaPPS16:MEH-PPV = 100:0.01:0.20 (w/w) (JF14) and LaPPS10:P(MMA-*co*-MMAnt):LaPPS16:MEH-PPV = 100:40:0.01:0.20 (w/w) (JF17). The difference between the blends JF14 and JF17 is the presence of the methacrylic copolymer in JF17 as the second major component. The addition of this copolymer brings about at least three important consequences: it greatly enhances the optical quality of the films; there is an improvement of the film adhesion on the substrate leading to more flat surfaces; and there is a relative decrease of the contribution of the β-phase still present from the blue emitter LaPPS10 (absorption and emission bands at 432 and 442 nm, respectively). Dilution effect in polymer blends has been observed in several systems leading to a separation of the polymer chains and to the decrease of interchain interactions [33,45–47]. Moreover, the contribution of the β-phase in the JF17 blend seems to be less important than in the JF14, indicating that the improved optical quality produced by the inclusion of the acrylic copolymer is associated to the film morphology.

Fig. 4 also depicts the photoluminescence spectra of the blends. Emission in the higher energy edge is characteristic of the LaPPS10, where the 0–0 band occurs at 442 nm and a second vibronic peak appears at 465 nm, the same observed for this individual polymer in Fig. 3. However, the vibronic ratio is not constant for the three systems in solid state: LaPPS10, JF14 and JF17 blends. The lower vibronic ratio I_{465}/I_{442} observed for blend JF14 can be explained by a dilution effect which reduces the homopolymer interchain resonant energy transfer, whereas the higher vibronic ratio I_{465}/I_{442} and the spectral broadening observed for the JF17 can be explained by the contribution to the emission of the P(MMA-*co*-MMAnt) acrylic copolymer. Finally, the broad band at 540 nm present in both blends can be assigned to a contribution of the emission of LaPPS10 and LaPPS16 aggregates, along with that of MEHPPV. It is worthwhile to note that the emission of this polymer is very sensitive to concentration. In diluted solution (Fig. 2(b)) it peaks at 554 nm, whereas in the film the emission redshifts to 605.8 nm (Fig. 3(b)). Literature data reports r redshiftings of 100 nm for blends of MEHPPV with PMMA from concentrations of 12.5% in relation to the pure polymer film [48]. When diluted in polyfluorene, the emission around 600 nm which appears as a shoulder in the blends containing 3% to 1%, is no longer detected when MEHPPV is present in the concentration of 0.4% [20]. This progressive MEH PPV redshifting with concentration is illustrated in Fig. 3(c). Therefore, the broad band of the PL emission extending from 520 to 600 nm (see inset in

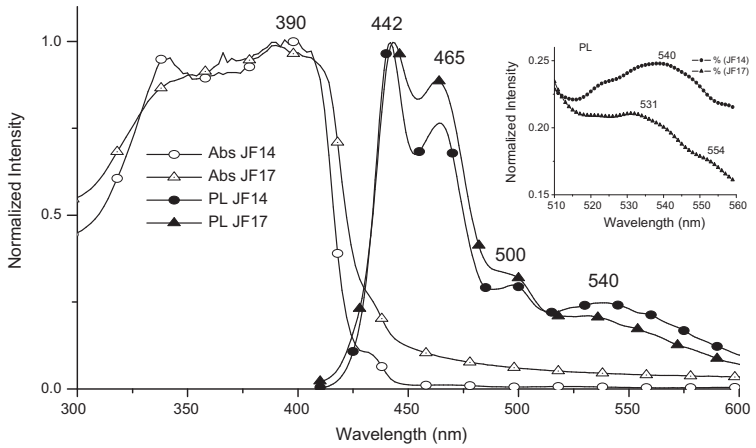

Fig. 4. Electronic absorption and emission spectra of blends JF14 and JF17 (λ_{exc} = 380 nm) in film form.

Fig. 4) can be attributed to the dopants LaPPS16 and MEH PPV, which do not appear separately due to their low concentration. It should be noted that the intensity in the region of 540 nm is higher for the JF14 than for JF17, characterizing a more efficient energy transfer in the former.

The spectral overlap among the absorption and emission of the blended components is a necessary condition for the resonant energy transfer from a donor polymer to an acceptor, which, in addition, also requires a close proximity between the components (distance within the Förster radium). Nevertheless, this condition must be avoided to some extent if a white emission is desired in a photoluminescent system. In other words, in a white emitting device, the resonant energy transfer process should not be completely efficient since the entire emission spectral range of white color must have contributions of the several chromatic components. Thus, from the photophysical point of view, to achieve white emission, only partial energy transfer processes and inner filter effects must be allowed in a photoluminescent system. Polymer blended systems with phase separation may undergo white emission because the domains are independent emissive sites, and the inner filter effect may be controlled by the thicknesses. Fig. 4 shows that the photoemission has a strong blue component, indicating that the energy transfer processes from the higher energy donors (LaPPS10 and P(MMA-*co*-MMAnt)) to the lower energy acceptors (LaPPS16 and MEH-PPV), are not complete suggesting that both blends underwent phase separation processes and the emission from the lower energy components are prevented by the inner filter, inhibiting their excitation.

In an attempt to explain the photoluminescence spectra observed for the two blends, we analyzed the morphology by epifluorescence optical microscopy. In Fig. 5a the morphology of the JF14 film under UV excitation (λ_{exc} = 330–380 nm, λ_{em} > 440 nm) is shown. A uniform blue emission over the entire samples is observed which is characteristic of LaPPS10, the major component, based on the emission spectra in Fig. 4. Nevertheless, more detailed images by combining the UV excitation with white lamp revealed also some blue spots of the LaPPS16 component (sizes smaller than 1 μm) (Fig. 5b) and under excitation with visible light (λ_{exc} = 480–500 nm, λ_{em} > 550 nm) red spots from the MEH-PPV component are the only one observed (Fig. 5c). Thus, the morphology of the JF14 blend can be described as a dispersion of the LaPPS16 and MEH-PPV domains in a blue matrix of LaPPS10. A phase separation is clearly seen. The morphology of the JF17 blend is completely different and since the only change is the addition of P(MMA-*co*-MMAnt), this is the responsible by the change. In Fig. 5d using UV excitation (λ_{exc} = 330–380 nm, λ_{em} > 440 nm), two types of blue domains can be seen: dispersed interconnected blue darker domains in a light blue matrix of LaPPS10. The dispersed domains are better visualized when with the combination of UV and white illumination (Fig. 5 – right side) and now, in addition to the interconnected domains we also identity dispersed spherical blue domains whose diameters are around 20 μm, which were ascribed to the P(MMA-*co*-MMAnt) (Fig. 5e). This combination also showed the presence of some interconnection of blue domains through a interphase, probably due to the LaPPS16 or some non-segregated P(MMA-*co*-MMAnt) components. Again the MEH-PPV red domains can be seen using visible light (λ_{exc} = 480–500 nm, λ_{em} > 550 nm) (Fig. 5f).

Therefore, from the morphological point of view, the components of these blends have a very low (if some) miscibility, forming a matrix of LaPPS10 and segregated domains of LaPPS16 and MEH-PPV in the case of JF14, and of LaPPS16, P(MMA-*co*-MMAnt) and MEH-PPV in the case of JF17. Even with phase separation, the acrylic copolymer played an important role on the film morphology, creating the possibility of interconnected domains formation in the JF17 blend. Nevertheless the changes of the photoluminescence spectra are not substantial. Because of this apparent poor miscibility in both JF14 and JF17 blends, we would not expect a complete energy transfer processes from the donors to the acceptors even though their absorption and emission are strongly overlapped. This result is an interesting example of the interplay between photophysical behavior and morphology. However, steady-state

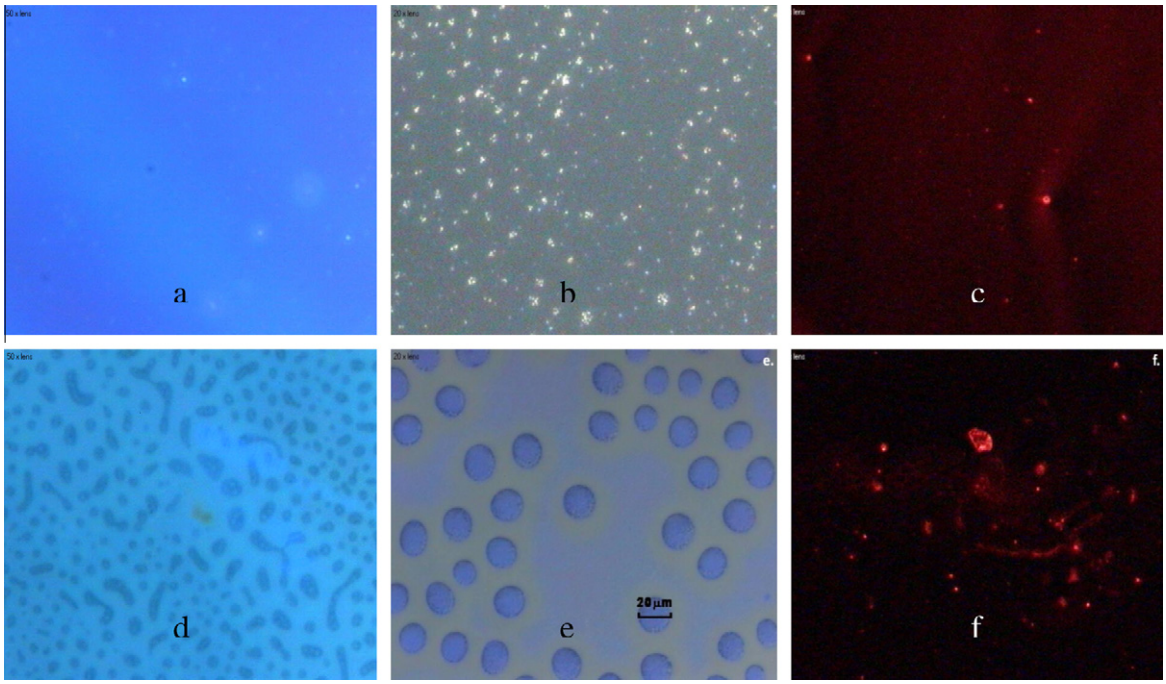

Fig. 5. Epifluorescence images of (a–c) JF14 and (d–f) JF17 and (d) UV excitation (λ_{exc} = 330–380 nm, λ_{em} > 440 nm); b and e (combining UV and white light to improve the contrast); c and f (λ_{exc} > 490 nm, λ_{em} > 550 nm). Amplification 22×.

fluorescence spectroscopy is not the most useful tool to evaluate the energy transfer processes when samples depict complex or overlapped emission spectra.

In order to get additional insight about the possibility of energy transfer processes from LaPPS10 and P(MMA-*co*-MMAnt) to LaPPS16 and MEH-PPV, fluorescence decays of the donors were measured in blends (in the presence of the acceptors), and compared these values with those of each isolated polymer in both solution and in film form. The LaPPS10 photoluminescence decays in degassed chloroform solution (10^{-5} mol L^{-1}) (λ_{exc} = 320 nm, λ_{em} = 440 nm) is bi-exponential with τ_1 = 0.48 ns (54%) and 0.79 ns (46%) (Table 1) and becomes mono-exponential in films with a lifetime of 0.31 ± 0.07 ns. This lifetime range is in accordance with those reported for polyfluorenes in diluted solution (from 0.08 to 5.0 ns) [36,49–52]. The decrease in lifetime in the solid state can be attributed to the formation of aggregates as well as to several possibilities of quenching processes in the solid state, apart from resonant energy transfer from disordered to β phases.

For the JF14 polymer blend in solution (λ_{exc} = 320 nm, λ_{em} = 440 nm), the decay is practically the same as the LaPPS10 in solution (bi-exponential with τ_1 = 0.48 ns (54%) and 0.76 ns (45%) (Table 1)), indicating that the presence of other components is not interfering with the LaPPS10 photophysics, and that no resonant energy transfer processes are occurring. Nevertheless, JF14 film exhibits a bi-exponential decay with the faster component of 0.41 ± 0.07 ns (86%), practically the same of the isolated LaPPS10 films and a longer component with τ_2 = 2.98 ± 0.01 ns with a smaller contribution (13%), that is absent in solution. Apart from a possible assignment of this longer decay to molecular aggregation in the ground state, as shown by the absorption and emission spectra, the complexity of the morphology makes the assignment of this transition very difficult.

Decays in JF17 blend-films, on the other hand, are mono-exponential, as also observed for solutions. Nevertheless, there is a pronounced decrease of the fluorescence lifetime in solid state (not observed in JF14) compared with the solution, which suggests that some non-radiative resonant energy transfer processes from LaPPS10 to the other components are occurring. It is very well documented in the literature that chain interpenetration favors the resonant energy transfer processes because the

Table 1
Fluorescence decays of the pure blend components in several conditions, using λ_{exc} = 320 nm, λ_{em} = 440 nm; *B* is the contribution of every lifetime to the entire decay, χ^2 measures the quality of the exponential fitting.

Materials	τ_1 (ns)	B_1 (%)	τ_2 (ns)	B_2 (%)	χ^2
LaPPS10 (solution)	0.48 ± 0.08	54	0.79 ± 0.06	46	1.041
LaPPS10 (film)	0.31 ± 0.07	100			1.089
P(MMA-*co*-MMAnt) (film) [22][c]	2.5	72	7.4	28	
JF14 (solution)	0.48 ± 0.07	55	0.76 ± 0.08	45	1.135
JF14 (film)[a]	0.41 ± 0,08	86	2.98 ± 0.01	13	1.161
JF17 (solution)[b]	0.62 ± 0.03	97			1.097
JF17 (film)	0.28 ± 0.08	97			1.080

[a] λ_{em} = 465 nm.
[b] λ_{em} = 410 nm.
[c] λ_{exc} = 370 nm, λ_{em} = 415 nm.

donor–acceptor distances approaches of that equivalent to the Förster radius [44]. This result can be correlated with the epifluorescence micrographs which showed the presence of interconnected domains that would lead to chain interpenetration. Based on this analysis we can conclude that the presence of the P(MMA-*co*-MMAnt) induces a better dispersion of the components, interferes with the interface energy, improves the optical quality of the films and facilitates the energy transfer from the donor to the acceptors.

3.2. Electroluminescence

Fig. 6 shows the electroluminescence spectra of LaPPS10 and of the JF14 and JF17 blends. The EL spectrum of LaPPS10 shows a band emission with vibronic structure, where the most intense band (0–0 band) is at 453.5 nm, 11 nm red-shifted as compared to the PL (Fig. 4). The vibronic progression occurred at 478.7 and 515.3 nm with a broad and less intense shoulder at 558 nm. It is particularly interesting that the relative intensities of the vibronic bands in the EL spectrum decrease at about half intensity on going the 0–0 to 0–1, from 0–1 to 0–2 and from the 0–2 to 0–3 vibronic bands which is completely different of the PL spectrum (Fig. 3), where systematic decrease of the emission was not observed. The EL spectrum is also sharper, showing, therefore, a better spectral resolution. These differences indicates that the EL is originated from other exciton species than those responsible for the PL. PL is originated from a very broad distribution of different species either by direct excitation or by several types of possible energy transfer processes. Moreover, considering the presence of the β-phase in the solid state identified by the sharper absorption band at 432 nm, red-shifted compared to the absorption of the amorphous disordered chains, and the emission band at 442 nm, we suggest that the EL is probably produced in the ordered β-phase of the LaPPS10.

Significant differences between EL and PL spectra were also observed for the JF14 and JF17 blends. The EL spectrum of the JF14 blend is similar to that of LaPPS10 in terms of spectral range, but significant differences were noted in the relative intensities of the red-edge peaks. The blue peak at 453 nm is present in all EL spectra (0–0 band of LaPPS10), but those at 514 nm (green) and 550–560 nm (yellow) were more intense, providing additional contribution to the visual color of the entire emission. The relative contributions of these red-edge peaks are greater in the EL compared with the PL spectra (Fig. 4). There are two possible explanations for the relatively more intense red-edge emission in EL. First, is that the excitation efficiency by photons in the PL is proportional to the amount of each component in the blend, in the absence of efficient energy transfer processes. Since we are using excitation in the blue region, the efficiency of the photoexcitation of the LaPPS16 and of the MEH-PPV are lower and thus their emissions are also relatively lower. This is not relevant for the EL spectrum. The second explanation is that the EL emission is proportional to the efficiency of the charge transport across each phase, to the charge recombination and to the efficiency of the exciton recombination. The first two processes are intrinsically associated with properties of each material and cannot be correlated with the PL. If they are more efficient for the LaPPS16 and for the MEH-PPV, it will be expected that the relative EL from these two components will be greater, as we effectively observed. Moreover, the band around 550–560 nm was attributed to the emission from the LaPPS16 aggregates, and again the EL seems to be more efficient at the more ordered crystalline phase of this polymer, as it does for LaPPS10. The EL is redshifted as compared to the PL, and that can be accounted for the charge trapping in the dopants domains, apart from energy transfer. The dopants emission in both JF14 and JF17 are enveloped the 500–700 nm region. In the EL spectrum of the JF14 blend a shoulder is seen at 590 nm which was attributed to the MEH-PPV domains, according to epifluorescence images. (See inset of Fig. 6). According to published data, the work function of the β phase regions is ca. 5.3 eV, i. e. 0.3 eV lower than that (5.65 eV) of the polyfluorene matrix [40], suggesting that hole carriers tend to be injected into the β phase rather than into the polyfluorene disordered matrix. It has been demonstrated that the β phase in poly(9,9-dioctylfluorene) is an energetically

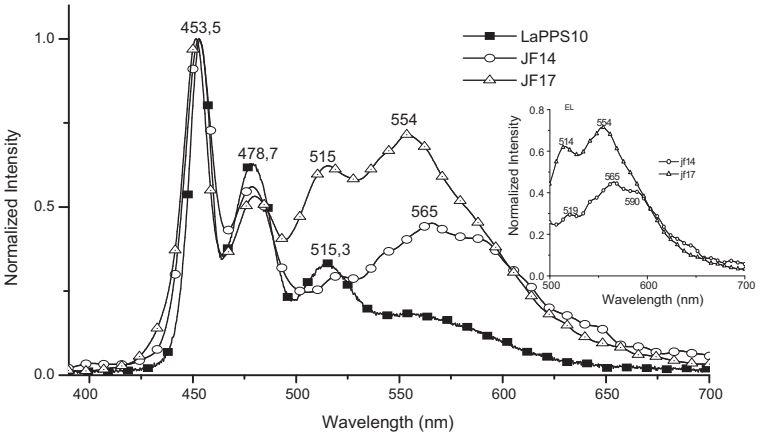

Fig. 6. EL spectra of the LaPPS10 film and JF14 and JF17 blends.

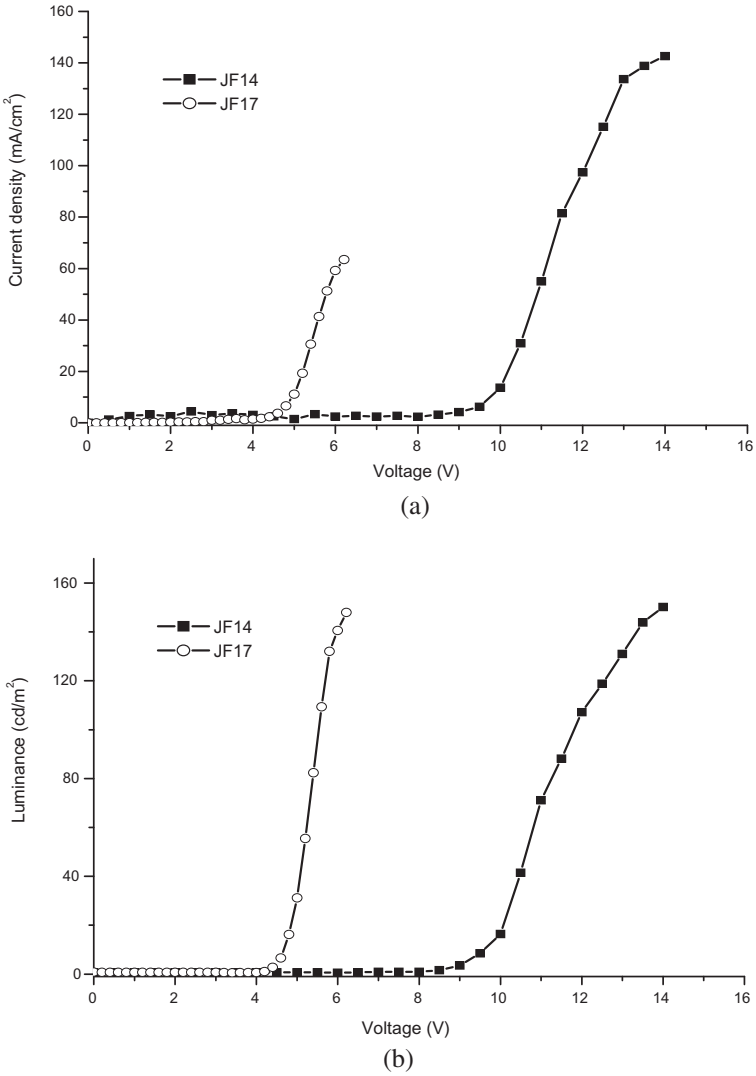

Fig. 7. (a) Current density × voltage and (b) luminance × voltage graphs of devices built with blends JF14 and JF17.

favorable environment for charge carriers, with an enhanced charge carrier mobility [53]. Due to its smaller band gap it can act also as traps for carriers, competing with other species in excitonic energy transfer processes, and more importantly, as carrier trapping/recombination sites.

The addition of P(MMA-*co*-MMAnt) in JF17 resulted in considerable differences in the EL profile as compared to LaPPS10 and JF14. There is a pronounced relative increase of the red-edge emission compared with the LaPPS10 and compared with the JF14. As previously mentioned, the EL emission is strongly correlated to the charge transport and charge recombination that seems to be enhanced by the addition of the acrylic copolymer. Taking into account the morphological and the photophysical properties, we can conclude that the formation of interconnected phases in JF17 are favoring not only the energy transfer processes (lifetime decreased) and the optical quality of the film but also the charge transport as already indicated for systems forming bulk heterojunctions [42]. Bulk heterojunctions are in JF17 enhancing the emission of LaPPS16, as indicated by the increase of the relative intensity of the bands at 515 and 554 nm. If the hypothesis of the heterojunction favoring the charge transport is correct, we should also expect changes on the electrical performance of these devices.

In the operation of an organic light-emitting diode (OLED) either the operating voltage or the luminance efficiency, depends firstly on the effective injection of carriers from both electrodes. It also strongly depends on the charge transport, the exciton generation and the recombination process. To achieve the lowest possible threshold voltage, the contact (cathode or anode) with the organic layer should approximate to ohmic condition. In general, this condition is easily reached with the anode, the transparent contact, in which the work function is close to the HOMO of the organic conjugated molecule. The injection of electrons, on the other hand, requires a more sophisticated technology to avoid the unbalance between electrons and holes.

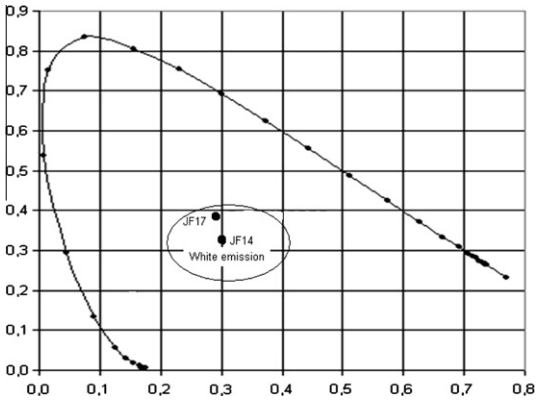

Fig. 8. CIE diagram relative to the electroluminescence of blends JF14 (0.30 and 0.32), JF17 (0.29 and 0.38).

In the present devices we used a simple structure, with a hole transport layer (PEDOT:PSS), and only one aluminum layer in the cathode (without an electron transport layer). Even so, both JF14 and JF17 devices showed a good performance as white OLED, as shown in Fig. 7. Fig. 7a shows the current–voltage curves for JF14 and JF17 devices, both exhibiting a diode characteristic. JF17 operates with lower voltage, having a threshold voltage below than 5 V and with a luminance, while the threshold voltage for JF14 was at about 10 V. Similar response was observed in the luminance vs. voltage curves. JF17 device reached 150 cd/m^2 at 6 V (60 mA/cm^2), while the JF14 presented the same luminance at 14 V (140 mA/cm^2). Therefore, the performance of JF17 was superior, since it achieved a luminance efficiency (cd/A) 2.5 higher, i.e. the same luminance at lower voltage and electric current. Fig. 8 exhibits the CIE coordinates of both devices (JF14 and JF17), and, as it can be seen in the CIE diagram, they emits in white region.

The HOMO and LUMO levels of the components used in the blends of JF14 and JF17 are shown in Table 2. The work functions of ITO and aluminum are about 4.8 and 4.1 eV, respectively. The values corresponding to LaPPS16 and MEHPPV were taken from Refs. [54,20], and those of poly(methyl methacrylate-*co*-methyl antracenyl methacrylate) were determined by cyclic voltammetry and UV–vis spectroscopy. The latter is in the same range of published data for poly(methyl methacrylate) copolymers with pendant chromophores: the reported HOMO and LUMO for the polymer with pendant azodyes are −6.08 and −3.21 eV, respectively [55].

Since the active layer of each luminescent diode is a blend composed by several components, it is not possible to sketch a sequence of energy barriers faced by the charge carriers, either for injection or transport mechanisms. The basic difference between JF17 and JF14 is that the blend of the former includes P(MMA- *co*-MMAnt), whose HOMO value is higher than the others. However, JF17 exhibited a better electrical and optical performance, as can be seen by the threshold voltage in the current and luminance curves (Fig. 7). Most probably this improvement brought about by P(MMA- *co*-MMAnt) to the blend is related to morphological modifications bringing the molecules in closer interactions one to another.

Table 2
HOMO and LUMO values in eV.

	PEDOT:PSS	P(MMA- *co*-MMAnt)	LaPPS10	LaPPS16	MEH-PPV
LUMO	3.50	3.90	2.60	3.04	2.80
HOMO	5.20	6.80	5.97	5.60	4.90

4. Conclusions

This study with the blends JF14 and JF17 showed that due to several mechanisms of energy transfer processes, an emission profile proportional the composition of every component is not the outcome of the device. The performance of the blends were compared, the segregated domains of the green and red emitters in the blue matrix brought about different behaviors. In the JF17 blend, the methacrylic non-conjugated copolymer was the predominant component in the dispersed phase, whereas for JF14 the MEH-PPV (red emitter polymer) was the main component of the domains. The differences in the EL and PL indicated that the mechanisms involved in the dynamics of excited states and/or in quenching processes are different in both cases. The EL emissions suggested that the cascade mechanism for the charge migration, charge recombination or energy transfer processes are incomplete, which opens possibility for more than one type of mechanism, resulting in emissions at different wavelengths. Spectroscopic data brought evidence of the formation of the β phase in the polyfluorene matrix, and due to differences in band gap, it was concluded that hole carriers tend to be injected into that phase rather than into the disordered one. The device with blend JF17 presented a better performance when compared with device JF14. Its turn on voltage was 4 V whereas that of JF14 was 9 V. The maximum luminance attained was 148 cd/m^2 at 6 V with current density maximum of 63 mA/cm^2 for JF17, compared to 142 cd/m^2 at 14 V for JF14.The behavior of the blue LED built with the pure matrix is inferior to those of the blends: turn on 13 V, maximum luminance 3.4 cd/m^2 at 20 V at 7.6 mA/cm^2. The CIE coordinates for EL emission of JF14 blend the coordinates are (0.30, 0.32) and for JF17 blend are (0.29, 0.38) corresponding to white light emission. It is worthwhile to note that these EL devices were not optimized; they were built in a standard configuration for comparison purposes, and focused in white light emission.

Acknowledgements

The authors are grateful to Dr.Paula C.Rodrigues for her contribution in the voltammetry measurements, and also to CNPq (Conselho Nacional de Pesquisas – Brazil), FAPESP (Fundação de Amparo à Pesquisa do Estado de São Paulo – Brazil) and National Institute on Organic Electronics (INEO/CNPq/FAPESP/CAPES) for financial support and fellowships.

References

[1] B.W. Andrade, S.R. Forrest, Adv. Mater. 16 (2004) 1585.
[2] L. Hou, L. Duan, J. Qiao, D. Zhang, G. Dong, L. Wang, Y. Qiu, Org. Electron. 11 (2010) 1344.

[3] D. Gupta, M.K. Deepak, Opt. Mater. 28 (2006) 295.
[4] J.M. Kang, M.J. Park, S.K. Kim, C. Lee, S.H. Jin, D.H. Hwang, Curr. Appl. Phys. 6 (2006) 756.
[5] J. Zou, J. Liu, H. Wu, W. Yang, J. Peng, Y. Cao, Org. Electron. 10 (2009) 843.
[6] B. Hu, F. Karasz, J. Appl. Phys. 93 (2003) 1995.
[7] Q.J. Sun, J.H. Hou, C.H. Yang, Y.F. Li, Y. Yang, Appl. Phys. Lett. 89 (2006) 153501.
[8] Q.L. Niu, Y.H. Xu, J.B. Peng, J. Lumin. 126 (2007) 531.
[9] J. Li, T. Sano, Y. Hirayama, K. Shibata, Synth. Met. 159 (2009) 36.
[10] A. Misra, P. Kumar, M.N. Kamalasanan, S. Chandra, Sci. Semicond. Technol 21 (2006) 35.
[11] M. Mazzeo, D. Pisignano, F. Della-Sala, J. Thompson, R.Y.R. Blyth, G. Gigli, R. Cingolani, G. Sotgiu, G.G. Barbarella, Appl. Phys. Lett. 82 (2003) 334.
[12] Q.J. Sun, B.H. Fan, Z.A. Tan, C.H. Yang, Y.F. Li, Y. Yang, Appl. Phys. Lett. 88 (2006) 163510.
[13] D.H. Hwang, J.H. Lee, J.I. Lee, C.H. Lee, Y.B. Kim, Mol. Cryst. Liq. Cryst. 405 (2003) 127.
[14] K.G. Ho, H.F. Meng, S.C. Lin, S.F. Horng, C.S. Hsu, L.C. Chen, S.M. Chang, Appl. Phys. Lett. 85 (2004) 4576.
[15] T.W. Lee, O.O. Park, H.N. Cho, J.M. Hong, C.Y. Kim, Synth. Met. 122 (2001) 437.
[16] Z. Tan, R. Tang, Q. Sun, C. Yang, F. Xi, Y. Li, Thin. Solid Films 516 (2007) 47.
[17] J.H. Park, T.W. Lee, Y.C. Kim, O.O. Park, J.K. Kim, Chem. Phys. Lett. 403 (2005) 293.
[18] G. He, Y. Li, J. Liu, Y. Yang, Appl. Phys. Lett. 80 (2002) 22.
[19] J.H. Park, O.O. Park, J.K. Kim, J.W. Yu, Y.C. Kim, Curr. Appl. Phys. 6 (2006) 640.
[20] F.Z. Shen, F. He, D. Lu, Z.Q. Xie, W.J. Xie, Y.G. Ma, B. Hu, Semicond. Sci. Technol. 21 (2006) 16.
[21] L. Akcelrud, Progr. Polym. Sci. 28 (2003) 875.
[22] J.F. Deus, M.L. Andrade, T.D.Z. Atvars, L. Akcelrud, Chem. Phys. 297 (2004) 177.
[23] X. Gong, D. Moses, A.J. Heeger, J. Phys. Chem. B 108 (2004) 8601.
[24] A.M. Assaka, P.C. Rodrigues, A.P.M. Oliveira, L. Ding, B. Hu, F.E. Karasz, L. Akcelrud, Polymer 45 (2004) 7071.
[25] J.I. Lee, H.Y. Chu, S.H. Kim, L.M. Do, T. Zyung, D.H. Hwang, Opt. Mater. 21 (2002) 205.
[26] J.F. Lee, S.L.C. Hsu, Polymer 50 (2009) 2558.
[27] Z.Y. Xie, Y. Liu, J.S. Huang, Y. Wang, C.N. Li, S.Y. Liu, J.C. Chen, Synth. Met. 106 (1999) 71.
[28] A. Dogariu, R. Gupta, A.J. Heeger, H. Wang, Synth. Met. 100 (1999) 95.
[29] J. Gmeiner, S. Karg, M. Meier, W. Rieb, P. Strohriegl, M. Schwoerer, Act. Polym. 44 (1993) 201.
[30] X.Y. Jiang, Z.L. Zhang, B.X. Zhang, W.Q. Zhu, S.H. Hong Xu, Synth. Met. 129 (2002) 9.
[31] G. Tu, Q. Zhou, Y. Cheng, L. Wang, D. Ma, X. Jing, F. Wang, Appl. Phys. Lett. 85 (2004) 2172.
[32] M. Granström, O. Inganäs, Appl. Phys. Lett. 68 (1996) 147.
[33] B. Nowacki, E. Iamazaki, A. Cirpan, F.E. Karasz, T.D.Z. Atvars, L. Akcelrud, Polymer 50 (2009) 6057.
[34] J.F. Deus, G.P. Souza, W.A. Corradini, T.D.Z. Atvars, L. Akcelrud, Macromolecules 37 (2004) 6938.
[35] M.L. Andrade, T.D.Z. Atvars, Macromolecules 37 (2004) 9096.
[36] A. Monkman, C. Rothe, S. King, F. Dias, in: U. Scherf, D. Neher (Eds.), Polyfluorenes, Advances in Polymer Science, vol. 212, Springer, Berlin, 2008, pp. 187–225.
[37] P.K. Lekha, E. Prasad, Chem. Eur. J. 16 (2010) 3699.
[38] M. Knaapila, M.J. Winokur, in: U. Scherf, D. Neher (Eds.), Polyfluorenes, Advances in Polymer Science, vol. 212, Springer, Berlin, 2008, pp. 293–318.
[39] M. Grell, D.D.C. Bradley, X. Long, T. Chamberlain, M. Inbasekaran, E.P. Woo, M. Soliman, Act. Polym. 49 (1998) 439.
[40] R.F. Cossiello, M.D. Susman, P.F. Aramendia, T.D.Z. Atvars, J. Lumin. 130 (2010) 415.
[41] J.R. Tozoni, F.E.G. Guimarães, T.D.Z. Atvars, B. Nowacki, L. Akcelrud, T.J. Bonagamba, Eur. Polym. J. 45 (2009) 2467.
[42] Y.C. Chang, C.C. Hsiao, T.H. Jen, J.L. Liao, A.C. Su, S.A. Chen, J. Chin. Chem. Soc. 57 (2010) 564.
[43] Nguyen, T.-Q.; Martini, I. B.; Liu, J.; Schwartz, B. J. J. Phys.Chem. B 104 (2000) 237.
[44] J.R. Lakowicz, Principles of Fluorescence Spectroscopy, Academic Press, New York, 1999.
[45] A. Babel, S.A. Jenekhe, Macromolecules 37 (2004) 9835.
[46] G.C. Oh, J.J. Yun, S.M. Park, S.H. Son, E.M. Han, H.B. Gu, S.H. Jin, Y.S. Yoon, Mol. Cryst. Liq. Cryst. 405 (2003) 43.
[47] R.F. Cossiello, A. Cirpan, F.E. Karasz, L. Akcelrud, T.D.Z. Atvars, Synth. Met. 158 (2008) 219.
[48] H.L. Chou, S.Y. Hsu, P.K. Wei, Polymer 46 (2005) 4967.
[49] J.F. Deus, A. Cirpan, F.E. Karasz, L. Akcelrud, Curr. Appl. Phys. 10 (2010) 365.
[50] H.P.M. Oliveira, R.F. Cossiello, T.D.Z. Atvars, L. Akcelrud, Quím. Nova 29 (2006) 286.
[51] R.F. Dias, J. Morgado, A.L. Maçanita, P.C. Costa, H.D. Burrows, A.P. Monkman, Macromolecules 39 (2006) 5854.
[52] H.L. Vaughan, F.M.B. Dias, A.P. Monkman, J. Chem. Phys. 122 (2005) 1492.
[53] P. Prins, F.C. Grozema, B.S. Nehls, T. Farrell, U. Scherf, L.D.A. Siebbeles, Phys. Rev. B 74 (2006) 113203.
[54] T.W. Lee, J.H. Park, O.O. Park, J. Lee, Y.C. Kim, Opt. Mater. 30 (2007) 486.
[55] L. Hua, L.J. Mei, L.N. Jun, X.Q. Feng, G.J. Feng, W.L. Hua, L.Z. Chang, Sci. China Chem. 53 (2010) 588.